

Investigation of Boundary Conditions for Vertical Displacement Events with NIMROD

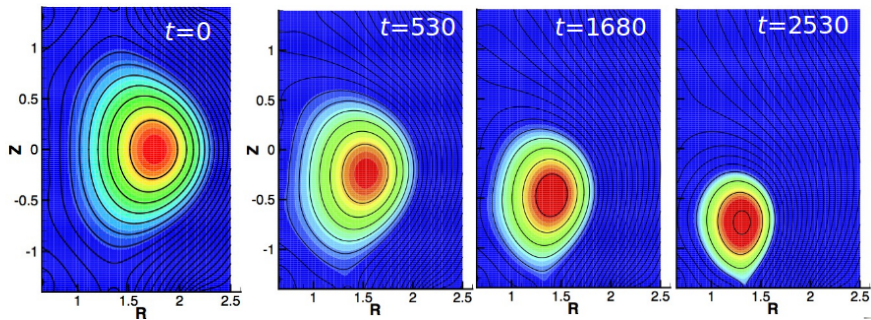
Sherwood 2018

K.J. Bunkers & C.R. Sovinec

University of Wisconsin-Madison

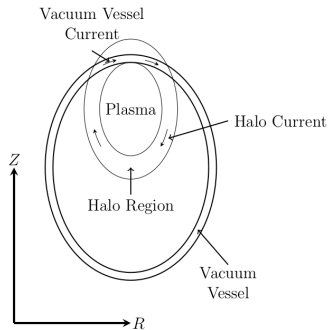
Vertical Displacement Events (VDEs) result from axisymmetric ideal instability with respect to vertical positioning.

- A VDE occurs when the plasma moves uncontrollably away from its equilibrium position into the containment vessel.
- Below is a series of snapshots (in Alfvén times) of the pressure (color) and poloidal flux (black lines) during a VDE in NIMROD.



VDEs have the potential to cause damage to tokamaks.

- VDEs can cause large wall forces through the interaction of induced currents and magnetic fields that damage the experiment.
- Several codes have calculated wall forces during VDE events, and there is still discussion about how the wall forces are mediated by the plasma-wall system.



We are applying the NIMROD code to help study integrated effects of VDEs.

- In these calculations, NIMROD is using a visco-resistive MHD model.
- NIMROD solves for the primitive fields (n , T , \mathbf{B} , \mathbf{V} , etc.); it does not use potentials.
- For spatial resolution, NIMROD uses spectral elements for the poloidal plane, and a Fourier decomposition in the periodic direction.
- NIMROD has two main time advance routines:
 - a (time-split) semi-implicit predictor/corrector algorithm.
 - a time-centered implicit leapfrog algorithm.

NIMROD solves the non-linear MHD equations.

$$\frac{\partial n}{\partial t} + \nabla \cdot (n\mathbf{V}) = \nabla \cdot (D_n \nabla n - D_h \nabla \nabla^2 n)$$

Continuity with diffusive numerical fluxes

$$mn \left(\frac{\partial}{\partial t} + \mathbf{V} \cdot \nabla \right) \mathbf{V} = \mathbf{J} \times \mathbf{B} - 2 \nabla(nT) - \nabla \cdot \overset{\leftrightarrow}{\Pi}$$

flow evolution

$$\frac{3}{2}n \left(\frac{\partial}{\partial t} + \mathbf{V} \cdot \nabla \right) T = -nT \nabla \cdot \mathbf{V} - \nabla \cdot \mathbf{q}$$

temperature evolution

$$\frac{\partial \mathbf{B}}{\partial t} = -\nabla \times (\eta \mathbf{J} - \mathbf{V} \times \mathbf{B}) + \kappa_B \nabla \nabla \cdot \mathbf{B}$$

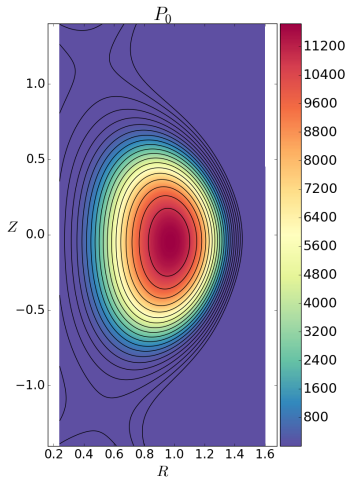
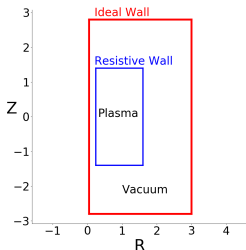
Faraday's/Ohm's Law with numerical error control

$$\mu_0 \mathbf{J} = \nabla \times \mathbf{B}$$

low- ω Ampere's law

A case from NSTX shared by M3DC¹ is being used to benchmark VDE behavior.

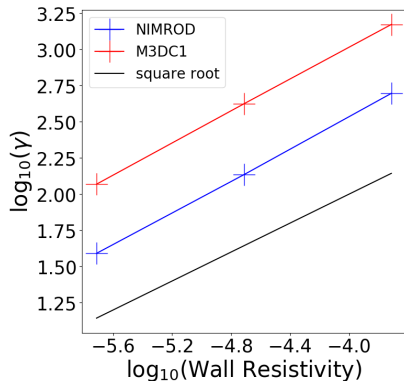
- The benchmark uses a rectangular mesh for the plasma and vacuum regions. The rectangular corners are of concern in NIMROD.
- The equilibrium is calculated from an EFIT file and re-solved with NIMEQ onto a NIMROD mesh.



Pressure contours with poloidal flux contour lines superimposed.

In the first attempt, NIMROD and M3DC¹ give different results for VDE linear growth rates.

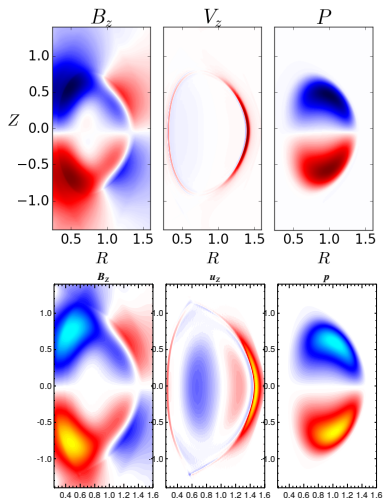
- The linear growth rates differed¹ from those given by M3DC¹ for $T_{\text{edge}} = 14.6$ eV.
- The cause of the difference between the observed growth rates is still unknown.
 - We are investigating whether the re-entrant corners are causing problems in the outer solution.



¹M3DC¹ data is from Krebs, private communication

The eigenfunctions for the linear calculations qualitatively agree.

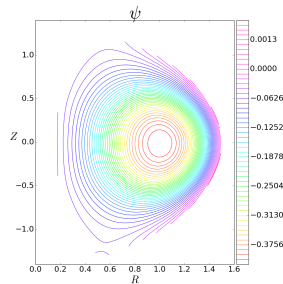
- The eigenfunctions are similar for NIMROD (top) and M3DC¹(bottom)².



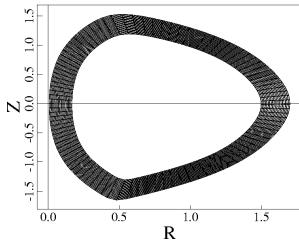
²M3DC¹ data is from Krebs, private communication

A flux aligned grid with conformal wall is helping us isolate the corner issue.

- The NSTX equilibrium is put into a flux aligned mesh using the same EFIT file as for the square calculations.
- The plasma region ψ looks like the image to the top right.
- These calculations have appeared to be VDE stable.
 - One possible reason is the conducting wall boundary condition can not be put as far away from the resistive wall as in the square cases.

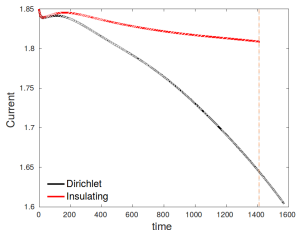


Finite Element Mesh

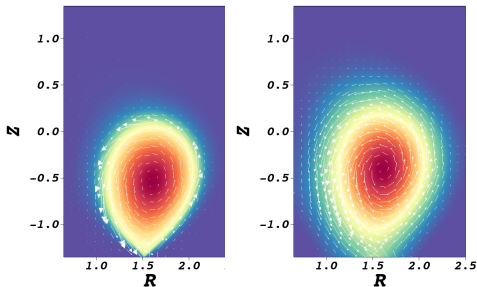


Sensitivity in the boundary conditions for VDE calculations suggests boundary modeling is important for VDE physics.

- This shows a computation of a VDE with and without insulating boundary conditions on temperature.
- The computation with Dirichlet conditions on T loses approximately 20% of its thermal energy over the first $1400\tau_A$.



Evolution of plasma current is sensitive to boundary conditions on T .



Contours of T with J vectors overlaid at $t = 1410$ with Dirichlet (left) and insulating (right).

More detailed modeling of sheath physics provides a set of boundary conditions that can be put in an MHD form.

- A sheath boundary condition model has been successfully developed for a fluid turbulence code.³
- The boundary conditions are formulated as being at the entrance to the magnetic presheath. They include a Chodura-Bohm velocity boundary condition.
 - The edge can be divided into presheath, magnetic presheath (MPS), and sheath regions.

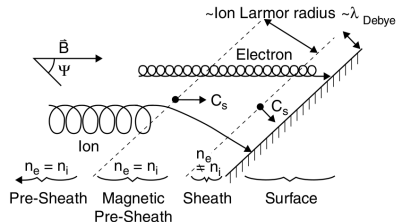


Figure of edge from Stangeby's *The Plasma Boundary of Magnetic Fusion Device* (2000).

³Loizu, Ricci, Phys. Plasm. **19** (2012) 122307

We can adopt the approach used by Loizu to find the boundary conditions.

- In the Loizu approach, the ion drift approximation (IDA) ($\frac{d}{dt} \ll \Omega_i$) is used to reduce the boundary conditions into an MHD usable form with the ion and electron momentum equations and continuity.
 - The IDA breaks down in the MPS and when formulated in a matrix equation, the determinant equals zero at the MPS entrance.
 - An ordering is imposed where derivatives along the wall are assumed to be order $\epsilon = \rho_s/L \ll 1$ with ρ_s the ion sound speed Larmor radius.
- MHD boundary conditions are deduced from the MPS entrance relations.
- Similar arguments of the breakdown of quasineutrality at the Debye sheath entrance can be used to find the Bohm criterion.⁴

⁴Riemann, J. Phys. D: Applied Phys. **24** (1991) 4 493

The singularities of the matrix equation yield the boundary conditions.

- We rewrite the continuity, ion momentum, and electron momentum equations into matrix form $\mathbf{M}\mathbf{x} = \mathbf{S}$ where \mathbf{S} represent sources that vanish as we get into the magnetic presheath. \mathbf{V} is the ion flow velocity, with the geometry shown below assuming adiabatic ions.

$$\begin{bmatrix} \hat{\mathbf{n}} \cdot \mathbf{V} & n \sin \alpha & -\frac{\cos \alpha}{B} \frac{\partial n}{\partial x} \\ \gamma T_i \sin \alpha & n m_i \hat{\mathbf{n}} \cdot \mathbf{V} & n \left(q_i \sin \alpha - \frac{m_i}{B} \cos \alpha \frac{\partial V_z}{\partial x} \right) \\ T_e \sin \alpha & 0 & n q_e \sin \alpha \end{bmatrix} \begin{bmatrix} \hat{\mathbf{n}} \cdot \nabla n \\ \hat{\mathbf{n}} \cdot \nabla V_z \\ \hat{\mathbf{n}} \cdot \nabla \phi \end{bmatrix} = \mathbf{S}$$

- $\det \mathbf{M} = 0$ then yields a relation that allows us to solve for \mathbf{V} .

The boundary equations that are derived are adapted to NIMROD.

- In the zeroth order ($\epsilon = \rho_s/L$) cold ion approximation, with \mathbf{V} the ion velocity and $c_s = \sqrt{T_e/m_i}$ the sound speed

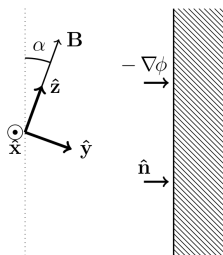
$$\boxed{\hat{\mathbf{n}} \cdot \mathbf{V}_{\text{wall}} = c_s \hat{\mathbf{n}} \cdot \hat{\mathbf{b}}_{\text{wall}}}, \quad \hat{\mathbf{n}} \cdot \nabla T_e = 0$$

$$\frac{T_e}{nq} \hat{\mathbf{n}} \cdot \nabla n = \hat{\mathbf{n}} \cdot \nabla \phi = -\frac{m_i c_s}{q} \hat{\mathbf{n}} \cdot \nabla(\mathbf{V} \cdot \hat{\mathbf{b}}) \sim 0$$

$$\hat{\mathbf{n}} \cdot \mathbf{J} = qnc_s \sin \alpha (1 - \exp[\Lambda - \eta])$$

- Here $\Lambda = \ln(\frac{m_i}{2\pi m_e})$ and η is the normalized potential relative to the wall.
- Strauss⁵ has considered sheath compatible boundary conditions and implemented a Neumann velocity boundary condition with effects similar to this Chodura-Bohm criterion.

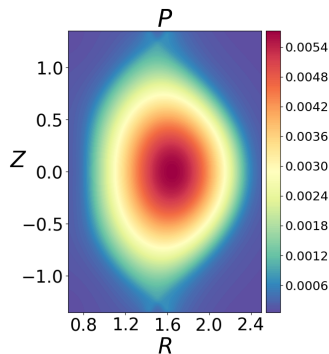
⁵Strauss, Phys. Plasm. **21** (2014) 032506.



Magnetic presheath coordinate directions.

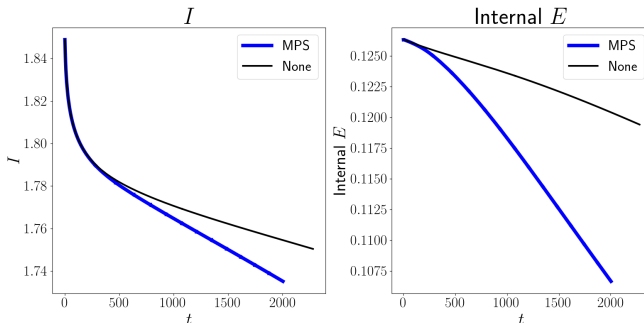
A generic tokamak equilibrium is used to demonstrate the magnetic presheath boundary condition.

- The figure on right shows the calculation area and pressure of the configuration.
- This begins from a double-null vertically symmetric equilibrium.
- This calculation was done without a resistive wall.
 - The equilibrium is vertically stable.



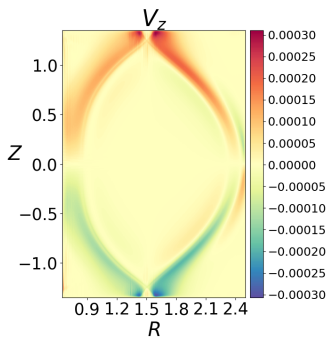
Applying the Bohm criterion with insulating temperature boundary conditions on the upper and lower boundaries leads to different behavior in current and internal energy.

- The current and internal energy began to diverge after approximately $1000\tau_A$. The internal energy separates much more than the current.
- In the figure MPS is the case where the Bohm criterion is applied on the top and bottom, and None applies to the no-slip velocity boundary condition .

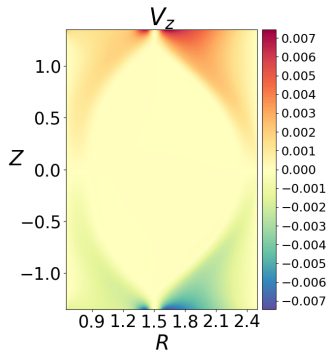


The flow velocity is also increased in the MPS boundary condition case.

- The velocity is primarily in the ϕ direction, but primarily in the Z direction in a poloidal cross section.
- The flows are approximately 10 times larger in the MPS applied case after 1200 Alfvén times.



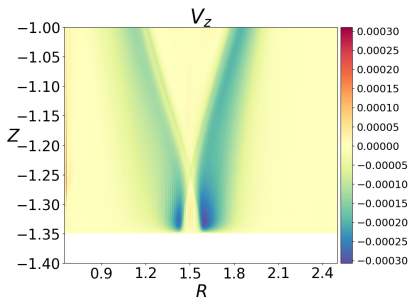
No MPS boundary conditions.



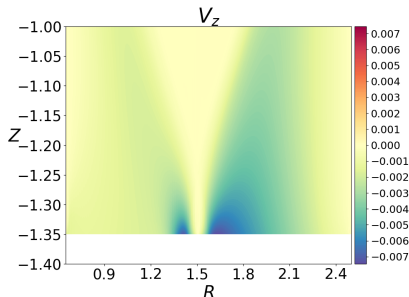
MPS boundary conditions.

The flow velocity is smoother towards the edges with this boundary condition.

- This is only enforcing $\hat{\mathbf{b}} \cdot \mathbf{V} = c_s$ at the wall with insulating temperature boundary conditions.
- The number density is diffused, and is not advected out of the system.



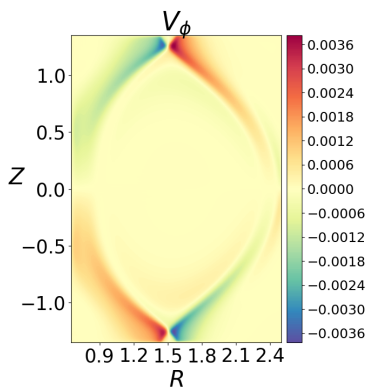
No MPS boundary conditions at $t \approx 1200\tau_A$.



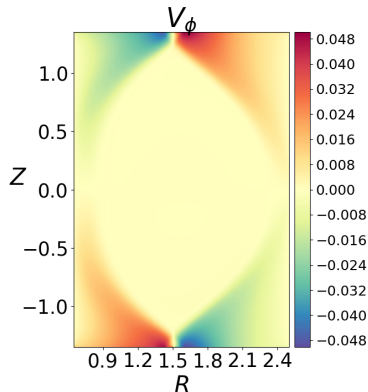
MPS boundary conditions at $t \approx 1200\tau_A$.

The toroidal component of flow velocity is also increased in the MPS boundary condition case.

- V_ϕ shows similar behavior to V_z with a 10-fold increase in velocity over the normal boundary conditions.



No MPS boundary conditions at $t \approx 1200\tau_A$.



MPS boundary conditions at $t \approx 1200\tau_A$.

- A VDE benchmark between NIMROD and M3DC¹ is making progress, but concerns with re-entrant corners in the outer region has slowed progress.
- A simple magnetic presheath (MPS) boundary condition has been tested in a tokamak equilibrium.
- The simple MPS condition has qualitative and quantitative differences from the usual no-slip and $\mathbf{E} \times \mathbf{B}$ velocity boundary conditions.

- Get the sheath boundary conditions working on a realistic unstable VDE case.
 - Implement the \mathbf{J} term on the boundary.
 - Use more than first-order accurate terms in the boundary condition.
 - Implement an electron temperature only insulating condition.
- Compare the linear VDE benchmark without square corners for the vacuum wall with M3DC¹.
 - Create a temperature offset for better comparisons with M3DC¹ for linear and nonlinear benchmarks.
- Fix the issue with the re-entrant corners.